Goos-Hänchen shift at Brillouin light scattering by a magnetostatic wave in the Damon-Eshbach configuration [Invited]

Yuliya Dadoenkova, Maciej Krawczyk, Igor Lyubchanskii

▶ **To cite this version:**

Yuliya Dadoenkova, Maciej Krawczyk, Igor Lyubchanskii. Goos-Hänchen shift at Brillouin light scattering by a magnetostatic wave in the Damon-Eshbach configuration [Invited]. Optical Materials Express, 2022, 12 (2), pp.717. 10.1364/OME.447984 . hal-03547737

HAL Id: hal-03547737
https://hal.science/hal-03547737

Submitted on 26 Mar 2022

HAL is a multi-disciplinary open access archive for the deposit and dissemination of scientific research documents, whether they are published or not. The documents may come from teaching and research institutions in France or abroad, or from public or private research centers.

L'archive ouverte pluridisciplinaire **HAL**, est destinée au dépôt et à la diffusion de documents scientifiques de niveau recherche, publiés ou non, émanant des établissements d'enseignement et de recherche français ou étrangers, des laboratoires publics ou privés.

Research Article | Vol. 12, No. 2 / 1 Feb 2022 / Optical Materials Express 717
Optical Materials EXPRESS

Goos-Hänchen shift at Brillouin light scattering by a magnetostatic wave in the Damon-Eshbach configuration [Invited]

YULIYA S. DADOENKOVA,[1] MACIEJ KRAWCZYK,[2] AND IGOR L. LYUBCHANSKII[3,4,*]

[1] *Lab-STICC (UMR 6285), CNRS, ENIB, Brest Cedex 3, 29238, France*
[2] *Institute of Spintronic and Quantum Information, Faculty of Physics, Adam Mickiewicz University in Poznań, Poznań, 61-614, Poland*
[3] *Donetsk Institute for Physics and Engineering named after O. O. Galkin (Branch in Kharkiv) of the National Academy of Sciences of Ukraine, Kyiv, 03028, Ukraine*
[4] *V. N. Karazin Kharkiv National University, Kharkiv, 61022, Ukraine*
[*] *ILyubchanskii@gmail.com*

Abstract: The lateral shift of an optical beam undergoing Brillouin light scattering by a spin wave propagating along the interface between magnetic and dielectric media (Damon-Eshbach configuration) in the total internal reflection geometry is studied theoretically. Linear and quadratic magneto-optic terms in polarization are taken into account. It is shown that the lateral shift depends on the polarization (*s*- or *p*-) state of the scattered electromagnetic wave as well as on the frequency of the spin wave.

© 2022 Optica Publishing Group under the terms of the Optica Open Access Publishing Agreement

1. Introduction

Phenomenon of the lateral shift at the reflection of an electromagnetic wave from the interface of two media in contrast to the laws of the geometric optics was predicted and observed for the first time by F. Goos and H. Hänchen at the glass-air interface in the forties of the 20th century [1] and nowadays is known as the Goos-Hänchen (GH) effect. Since that, various applications of this effect have been proposed, including chemical and temperature sensors [2–4], optical switches [5] and de/multiplexers [6]. The GH effect is well studied in linear optics [7,8], including magneto-optics where this phenomenon has been investigated theoretically and numerically [9–17] and observed in experiments [18]. The lateral beam shift was also studied for acoustic waves (Schoch effect) [19] and spin waves [20,21] (or their quasi-particle dual equivalents, phonons and magnons, respectively). The GH effect is common for the wave processes not only in optics, acoustics and spin wave dynamics, but also for reflection of electrons [22] and neutrons [23] because these particles can be presented as electronic and neutron waves.

In the case of three-wave interaction, GH effect has been studied for optical second harmonic generation [24,25] and for inelastic, or Brillouin light scattering (BLS) by acoustic phonons [26]. Nowadays BLS is used as very powerful tool for the study of different kind of elementary excitations in condensed matter physics including magnetic excitations, or spin waves [27–33]. Interaction between the electric field of an electromagnetic wave and the magnetization vector M of the medium in the phenomenological approach can be described via magnetization-dependent part of the dielectric permittivity tensor [34]. Contribution of the static part of M into permittivity leads to such magneto-optic (MO) phenomena as Faraday and Kerr effects (rotation of the polarization plane of the transmitted or reflected electromagnetic wave, respectively), as well to the magnetic birefringence [34], whereas the dynamic (time-dependent) part of the magnetization $\Delta\mathbf{m}$ is responsible for the BLS (or inelastic light scattering) by spin waves.

#447984 https://doi.org/10.1364/OME.447984
Journal © 2022 Received 15 Nov 2021; revised 4 Jan 2022; accepted 11 Jan 2022; published 26 Jan 2022

Optical Materials EXPRESS

It should be expected that the GH effect will take place in the case of BLS by spin waves. The description of this effect can be done similarly to approach used in our paper [26] where we described the GH shift at BLS by sound (acoustic phonons). However, in contrast to acousto-optics, for MO interaction we can consider contributions of magnetic subsystem to the polarization which are linear and quadratic on magnetization [34].

In this paper, we investigate the GH effect which occurs at BLS by spin waves at the interface between a magnetic film of yttrium-iron garnet (YIG) and a dielectric substrate of gadolinium-gallium garnet (GGG). We study the case of transversal MO configuration when the static magnetization is perpendicular to the incidence plane [34] and a spin wave propagates in YIG close to the YIG/GGG interface, which corresponds to the Damon-Eshbach configuration. In this configuration, the spin-wave propagation direction is perpendicular to the static magnetization orientation. This type of spin waves has surface character and its amplitude localization, at the top or bottom surface of the magnetic film, changes with the change of the propagation direction [35–37].

2. General equations

We assume that an electromagnetic wave of fundamental frequency ω and fundamental wavelength λ_0 (in vacuum) is incident from YIG on GGG under the incidence angle ω. The interface between the media is parallel to the x-axis, and (xz) is the incidence plane. A spin wave of the angular frequency Ω propagates along the x-axis, as shown in Fig. 1. The incident light wave interacts with the spin wave, and the scattered electromagnetic wave of the frequency $\omega \pm \Omega$ undergoes a lateral GH shift Δx.

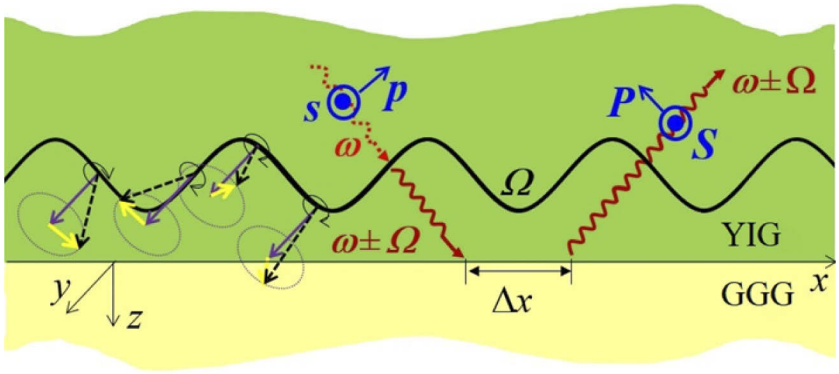

Fig. 1. Schematics of the BLS by a spin wave. Here s (S) and p (P) denote the incident (scattered) s- and p-polarized light, ω and Ω are the fundamental light angular frequency and the angular frequency of the spin wave, respectively, and Δx is the GH shift of the scattered electromagnetic wave. The violet and yellow arrows show the static m0 and the dynamic $\Delta\mathbf{m}$ parts of the magnetization vector $\mathbf{M}$ (black dashed arrow) which precesses around the y-axis.

Propagation of an electromagnetic wave with the angular frequency ω in YIG is described by the solution of the wave equation [38]

$$\nabla \times \nabla \times \mathbf{E}(\mathbf{r}, t) + \frac{\varepsilon_1 \mu_1}{c} \frac{\partial^2 \mathbf{E}(\mathbf{r}, t)}{\partial t^2} = -\mu_0 \frac{\partial^2 \mathbf{P}(\mathbf{r}, t)}{\partial t^2}, \tag{1}$$

where $\mathbf{E}(\mathbf{r},t)$ is the electric field of optical wave, ε_1 and μ_1 are the crystallographic dielectric permittivity and magnetic permeability of YIG, respectively, c is the speed of light in vacuum, μ_0 is the vacuum permeability, and $\mathbf{P}(\mathbf{r},t)$ is polarization vector.

Optical Materials EXPRESS

Taking into account both linear and quadratic MO interactions, electric polarization vector has the following form [34]:

$$P_i = if_{ijk}E_j m_k + g_{ijkl}E_j m_k m_l, \tag{2}$$

where f_{ijk} and g_{ijkl} are linear and quadratic MO tensors. For materials with cubic symmetry (such as YIG) these MO tensors have the following non-zero components:

$$\begin{aligned} &f_{xyz} = f_{yzx} = f_{zxy} = -f_{xzy} = -f_{yxz} = -f_{zyx} = f, \\ &g_{xxxx} = g_{yyyy} = g_{zzzz} = g_{11}, \\ &g_{xxyy} = g_{xxzz} = g_{yyxx} = g_{yyzz} = g_{zzxx} = g_{zzyy} = g_{12}, \\ &g_{xyxy} = g_{xzxz} = g_{yxyx} = g_{yzyz} = g_{zxzx} = g_{zyzy} = g_{xyyx} = \\ &= g_{xzzx} = g_{yxxy} = g_{yzzy} = g_{zxxz} = g_{zyyz} = g_{44}. \end{aligned} \tag{3}$$

It should be noted, that to simplify the analysis, we neglect the dependence of the magnetic permeability of YIG on the magnetization and assume $\mu_1 = \mu_0$. Indeed, the value of linear MO tensor element (gyromagnetic coefficient) of YIG is one order of magnitude less than the gyroelectric coefficient f [39].

The reduced magnetization vector $\mathbf{m} = \mathbf{M}/|\mathbf{M}|$ in YIG is decomposed into the static part $\mathbf{m}_0$ and the dynamic part $\Delta\mathbf{m}(\mathbf{r}, t)$ as:

$$\begin{aligned} &\mathbf{m} = \mathbf{m}_0 + \Delta\mathbf{m}(\mathbf{r}, t), \quad (\mathbf{m}_0, \Delta\mathbf{m}) = 0, \\ &\Delta\mathbf{m}(\mathbf{r}, t) \sim \exp(i\mathbf{q}\cdot\mathbf{r} - i\Omega t), \end{aligned} \tag{4}$$

where $\mathbf{q}$ and Ω are wave vector and frequency of the Damon-Eshbach spin-wave modes, respectively [35–37]:

$$\Omega^2 = \left(\omega_H + \frac{\omega_M}{2}\right)^2 - \left(\frac{\omega_M}{2}\right)^2 \exp(-2qd), \tag{5}$$

in the magnetostatic approximation [36], with $\omega_H = \gamma\mu_0 H_0$ and $\omega_M = \gamma\mu_0 M_0$, where $\gamma = 178$ rad·GHz/T is the gyromagnetic ratio, H_0 is the amplitude of the external magnetic field, and $M_0 = |\mathbf{M}|$ is the saturation magnetization, q is the wave number of the spin wave, and d is the YIG film thickness.

We will consider transverse MO configuration, when (xz) is the incidence plane, and the static magnetization vector $\mathbf{m}_0 = \{0, m_{0y}, 0\}$ is along the positive direction of the y-axis, *i.e.* $m_{0y} > 0$. Thus, according to Eq. (4), the dynamic magnetization vector can be written as $\Delta\mathbf{m}(\mathbf{r}, t)$ $\{\Delta m_x, 0, \Delta m_z\}$. In what follows, we assume $\{\Delta m_x, \Delta m_z\} << m_{0y}$.

In this case, the polarization of the incident and reflected light, which depends on the static magnetization, writes:

$$\begin{aligned} P_x &= -if m_{0y}E_z + g_{12}(m_{0y})^2 E_x, \\ P_y &= g_{11}(m_{0y})^2 E_y, \\ P_z &= if m_{0y}E_x + g_{12}(m_{0y})^2 E_z. \end{aligned} \tag{6}$$

The amplitude of the electromagnetic wave modulated by the spin wave due the MO interaction can be found as a solution of wave equation with the polarization at the combined frequencies:

$$\nabla\times\nabla\times\mathbf{E}(\mathbf{r}, t) + \frac{\varepsilon_1}{c}\frac{\partial^2\mathbf{E}(\mathbf{r}, t)}{\partial t^2} = -\mu_0\frac{\partial^2\Delta\mathbf{P}(\mathbf{r}, t)}{\partial t^2}. \tag{7}$$

Optical Materials EXPRESS

The polarization modulated by the magnetization oscillations has the following components (neglecting the terms containing $(\Delta m_x)^2$ and $(\Delta m_z)^2$ since they are much less than $(m_{0y})^2$):

$$\begin{aligned}\Delta P_x &= (if\Delta m_z + 2g_{44}m_{0y}\Delta m_x)E_y,\\ \Delta P_y &= if(E_z\Delta m_x - E_x\Delta m_z) + 2g_{44}m_{0y}(E_z\Delta m_z + E_x\Delta m_x),\\ \Delta P_z &= (-if\Delta m_x + 2g_{44}m_{0y}\Delta m_z)E_y,\end{aligned} \tag{8}$$

Taking the Fourier transform of Eq. (7) with respect to time and using the slowly varying envelope approximation [38], where $\mathbf{K}_{\omega\pm\Omega}\cdot\nabla\mathbf{E}(\mathbf{r},\omega\pm\Omega)>>\Delta\mathbf{E}(\mathbf{r},\omega\pm\Omega)$, we obtain the following reduced form of the wave equation for the BLS process:

$$\mathbf{K}_{\omega\pm\Omega}\cdot\nabla\mathbf{E}(\mathbf{r},\omega\pm\Omega) = -2i\frac{\omega^2}{c^2}\Delta\mathbf{P}(\mathbf{r},\omega\pm\Omega)\exp(i\mathbf{K}_{\omega\pm\Omega}\mathbf{r}) \tag{9}$$

with $\mathbf{K}_{\omega\pm\Omega}$ being the wave vector of the scattered electromagnetic wave at frequency $\omega\pm\Omega$.

The electric field components $E_i^{sc}(\omega\pm\Omega)$ $(i=x,y,z)$ of the scattered electromagnetic wave can be obtained from the corresponding polarization terms through the following equation:

$$E_i^{sc}(\omega\pm\Omega) = \frac{i\omega^2}{2c^2K_{\omega\pm\Omega}}\left(\frac{1}{V}\int_V P_i(\omega\pm\Omega)e^{i\mathbf{Q}\cdot\mathbf{r}}\,dr\right). \tag{10}$$

where $\mathbf{Q}=\mathbf{k}_\omega+\mathbf{q}-\mathbf{K}_{\omega\pm\Omega}$ is the wave vectors mismatch.

Using Eq. (1) and boundary conditions, the amplitudes of the reflected s- and p-polarized fundamental electromagnetic wave $E^{ref(s,p)}$ can be related to those of the incident wave $E^{inc(s,p)}$ using the corresponding reflection coefficients:

$$R^{(s)} = -\frac{k_{2z}+C_-^{(s)}}{C_+^{(s)}+k_{2z}}, \tag{11a}$$

$$R^{(p)} = \frac{k_{2z}/\varepsilon_2 - C_-^{(p)}}{C_+^{(p)} - k_{2z}/\varepsilon_2}, \tag{11b}$$

with

$$C_\pm^{(s)} = \pm\frac{k_{1z,\omega}^{(s)}}{\mu_1}, \tag{11c}$$

$$C_\pm^{(p)} = -\frac{if m_{0y}\mu_1 \pm k_{1z,\omega}^{(p)}k_x}{\varepsilon_1^{(p)}k_x \pm if m_{0y}k_{1z,\omega}^{(p)}}. \tag{11d}$$

Here k_x is the component of the wave vector along the x-axis, $k_{1z,\omega}^{(s,p)}$ and k_{2z} are the z-components of wave vectors in YIG and GGG, respectively:

$$k_{1z,\omega}^{(s)} = \sqrt{-k_x^2+\mu_1\varepsilon_1^{(s)}k_0^2}, \quad \varepsilon_1^{(s)} = \varepsilon_1 + g_{11}(m_{0y})^2, \tag{12a}$$

$$k_{1z,\omega}^{(p)} = \sqrt{-k_x^2+k_0^2\mu_1\left(\varepsilon_1^{(p)} - \frac{(fm_{0y})^2}{\varepsilon_1^{(p)}}\right)}, \quad \varepsilon_1^{(p)} = \varepsilon_1 + g_{12}(m_{0y})^2, \tag{12b}$$

$$k_{2z} = \sqrt{-k_x^2+\varepsilon_2 k_0^2}, \tag{12c}$$

where $k_0 = 2\pi/\lambda_0$ is the wavenumber in vacuum, and ε_2 is the dielectric permittivity of GGG.

Optical Materials EXPRESS

Using Eqs. (9)– (11), one can relate the amplitudes of the scattered electromagnetic wave to those of the incident.

The components of P-polarized scattered wave write:

$$E_x^{\mathrm{sc}}(\omega \pm \Omega) = \frac{1}{K_{\omega\pm\Omega}^{(P)}}(if\Delta m_z + 2g_{44}m_{0y}\Delta m_x)R^{(s)}E_y^{\mathrm{inc}}(\omega), \tag{13a}$$

$$E_z^{\mathrm{sc}}(\omega \pm \Omega) = \frac{1}{K_{\omega\pm\Omega}^{(P)}}(-if\Delta m_x + 2g_{44}m_{0y}\Delta m_z)R^{(s)}E_y^{\mathrm{inc}}(\omega). \tag{13b}$$

In what follows, we assume the amplitudes of the spin wave to be equal: $\Delta m_x = \Delta m_z = \Delta m$. In this case, the amplitude of the scattered P-polarized electromagnetic wave $E^{\mathrm{sc}(P)} = \sqrt{\left(E_x^{(\mathrm{sc})}\right)^2 + \left(E_z^{(\mathrm{sc})}\right)^2}$ is related to the amplitude of the s-polarized incident electromagnetic wave $E_y^{\mathrm{inc}} = E^{\mathrm{inc}(s)}$:

$$E^{\mathrm{sc}(P)}(\omega \pm \Omega) = \frac{\sqrt{2}\Delta m}{K_{\omega\pm\Omega}^{(p)}}\sqrt{(if)^2 + (2g_{44}m_{0y})^2}R^{(s)}E_y^{\mathrm{inc}}(\omega). \tag{14}$$

The component of the S-polarized scattered electromagnetic wave $E_y^{\mathrm{sc}} = E^{\mathrm{sc}(s)}$ has the following form:

$$E_y^{\mathrm{sc}}(\omega \pm \Omega) = \frac{\Delta m}{K_{\omega\pm\Omega}^{(s)}}[E_x^{\mathrm{ref}}(-if + 2g_{44}m_{0y}) + E_z^{\mathrm{ref}}(if + 2g_{44}m_{0y})], \tag{15}$$

where superscript (Ref.) refers to the reflected light of the fundamental frequency.

The components of the reflected electromagnetic wave E_x^{ref} and E_z^{ref} can be related to the amplitude of the incident electromagnetic wave using Maxwell's equations in the MO medium Eq. (1). Thus, the amplitude of S-polarized scattered electromagnetic wave is related to the amplitude of p-polarized incident fundamental wave as:

$$E^{\mathrm{sc}(S)}(\omega \pm \Omega) = \frac{\Delta m}{K_{\omega\pm\Omega}^{(s)}}[C_+^{(p)}(-if + 2g_{44}m_{0y}) + \tilde{C}_+^{(p)}(if + 2g_{44}m_{0y})]R^{(p)}E^{\mathrm{inc}(p)}, \tag{16}$$

where

$$\tilde{C}_\pm^{(p)} = \frac{\left(k_{1z,\omega}^{(p)}\right)^2 - \mu_1\varepsilon_1^{(p)}k_0^2}{\varepsilon_1^{(p)}k_x \pm if m_{0y}k_{1z,\omega}^{(p)}}, \tag{17}$$

Using Eqs. (14) and (16), one can write the scattered functions $\tilde{R}^{(S,P)}(k_x)$ which relates the amplitudes of the scattered S and P-polarized electromagnetic wave to those of the p- and s-polarized incident electromagnetic wave as:

$$\tilde{R}^{(S)} = \frac{E^{\mathrm{sc}(S)}(\omega \pm \Omega)}{E^{\mathrm{inc}(p)}(\omega)}, \tag{18a}$$

$$\tilde{R}^{(P)} = \frac{E^{\mathrm{sc}(P)}(\omega \pm \Omega)}{E^{\mathrm{inc}(s)}(\omega)}. \tag{18b}$$

Optical Materials EXPRESS

Assuming an incident Gaussian beam of waist w_0, the spatial profiles of the reflected $E^{\mathrm{ref}}(x)$ and scattered $E^{\mathrm{sc}}(x)$ beams can be calculated as:

$$E^{\mathrm{ref}\,(s,p)}(x) = \frac{1}{\sqrt{\pi}} \int_{-\infty}^{\infty} \tilde{E}^{\mathrm{inc}(s,p)}(K) R^{(s,p)}(\mathrm{K} + k_c) \exp(iKx) dK,$$
$$E^{\mathrm{sc}\,(S,P)}(x) = \frac{1}{\sqrt{\pi}} \int_{-\infty}^{\infty} \tilde{E}^{\mathrm{inc}(s,p)}(K) \tilde{R}^{(S,P)}(\mathrm{K} + k_c) \exp(iKx) dK, \tag{19}$$
$$\tilde{E}^{\mathrm{inc}(s,p)}(K) = \int_{-\infty}^{\infty} E^{\mathrm{inc}(s,p)}(x) \exp(-iKx) dx,$$

where k_c is the central wave vector of the incident beam and $K = k_x - k_c$.

3. Results of numerical calculations

For the numerical calculations, we take the following values of the parameters of YIG at the fundamental wavelength in vacuum $\lambda_0 = 1.15$ μm: $\varepsilon_1 = 4.58$, $f = -2.47 \cdot 10^{-4}$, $g_{11} = 2.89 \cdot 10^{-4}$, $g_{12} = 10^{-4}$, $2g_{44} = 2.31 \cdot 10^{-4}$ [39]. The relative dielectric permittivity of GGG is $\varepsilon_2 = 3.76$ [39]. Thus, the refractive indices of YIG along the s and p directions $n_1^{(s)} = |k_\omega^{(s)}|/k_0$ and $n_1^{(p)} = |k_\omega^{(p)}|/k_0$ are larger than the refractive index of GGG $n_2 = \sqrt{\varepsilon_2}$, and thus the total internal reflection of electromagnetic waves takes place at YIG/GGG interface at the incidence (critical) angles $\theta_{cr}^{(s)} = \arcsin(n_2/n_1^{(s)}) = 65.0225°$ and $\theta_{cr}^{(p)} = \arcsin(n_2/n_1^{(p)}) = 65.0243°$ for s- and p-polarization states, respectively. We limit our consideration to the total internal reflection geometry only, since it has been shown that at the light reflection at a single interface the GH shift is maximal at the incidence angles around the critical angle [1].

The static component of the magnetization vector in YIG, according to the approximation used here, is $m_{0y} \approx 1$, which is provided by the external magnetic field applied along the y-axis with the amplitude equal to the saturation magnetization of YIG: $H_0 = M_0 = 0.194 \cdot 10^6$ A/m [39]. It should be noted that to saturate a thin film in-plane (if there is no anisotropy, as in the case considered here), even smaller external field is sufficient, so that in practice H_0 can be less than M_0. The dynamic magnetization components in YIG are $\Delta m_z = \Delta m_x = 0.1$. The angular frequency of the spin wave is then $\Omega = 2\pi \cdot 20$ rad·GHz.

The waist of the incident electromagnetic beam is taken $w_0 = 100\lambda_0$. This choice is related to one of the characteristics of a Gaussian beam – the Rayleigh length $z_R = k_0 w_0^2/2$. At the distances below z_R, the divergence of the beam can be neglected. With the chosen values of w_0 and λ_0, z_R is about 3.6 cm, which is a realistic dimension for experimental setups.

First, we analyze the beam envelopes of the reflected and scattered light as functions of the incidence angle θ, as shown in Fig. 2. The shape and the amplitude of the *reflected* beam envelope is different for s- and p-polarized light when the incidence angle is less than the critical angles (see Figs. 2(a) and 2(b)). The GH shift, defined as the position of the maximum of that envelope relatively to the position of the maximum of the incident beam ($x = 0$), reaches the maximum around the critical angle whatever the polarization state of light is. The amplitudes of the *scattered* light are four orders of magnitude less than those of the reflected one. The amplitude of the P-polarized scattered light is about five times larger than that of the S-polarized scattered light. It should be noted that the shapes of the beam envelopes of s-polarized (p-polarized) reflected and P-polarized (S-polarized) scattered beams are similar due to the MO properties of YIG (see Eqs. (13)– (15) and discussion between). Thus, the GH shift takes place for both reflected and scattered electromagnetic waves.

Optical Materials EXPRESS

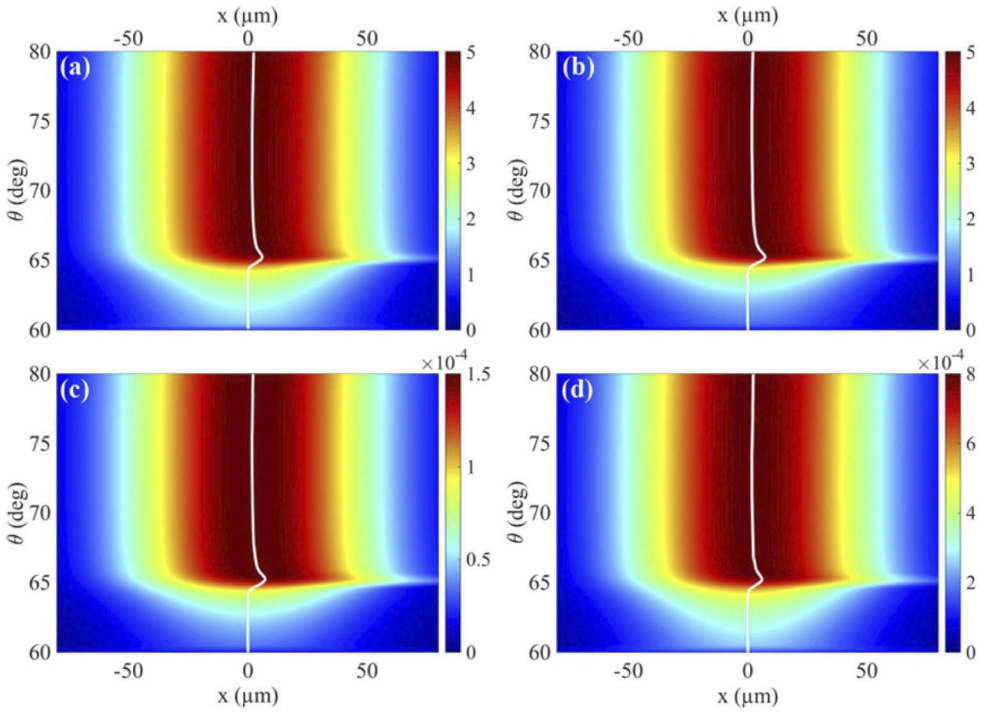

Fig. 2. The absolute value of the electric field (in V/m), or beam envelope, of the reflected light (top panel) and scattered light (bottom panel) of *s*-polarization (panels (a) and (c)) and *p*-polarization (panels (b) and (d)) as a function of the incidence angle θ and the *x*-coordinate. The white lines show the position of the maximum of the field relatively to the center of the incident beam (at $x = 0$).

Figure 3 compares the GH shifts of the reflected and scattered light. The lateral shift of *s*-polarized reflected light $\Delta x_s^{(\mathrm{ref})} \approx 6\,\mu\mathrm{m}$ (or 5.2 wavelength λ_0 in vacuum) is smaller than the GH shift of the *S*-polarized scattered light $\Delta x_S^{(\mathrm{sc})} \approx 7.5\,\mu\mathrm{m}$ ($6.5\lambda_0$), as shown in Fig. 3(a). On the contrary, the GH shift of the *P*-polarized scattered electromagnetic wave $\Delta x_P^{(\mathrm{sc})} \approx 6\,\mu\mathrm{m}$ ($5.2\lambda_0$) is smaller than that of the *p*-polarized reflected beam $\Delta x_p^{(\mathrm{ref})} \approx 7.3\,\mu\mathrm{m}$ ($6.35\lambda_0$), see Fig. 3(b).

In magnetic systems, the optical properties depend on the direction of the external magnetic field $\mathbf{H}_0$. The reversal of $\mathbf{H}_0$ (and thus the reversal of the static magnetization $\mathbf{m}_0$, so that it is directed antiparallel to the *y*-axis in the transverse MO configuration, *i.e.* $m_{0y} = -1$) does not affect the reflection coefficient $R^{(s)}$ of the s-polarized light because it depends on the square of the magnetization component, $(m_{0y})^2$ (see Eqs. (11a), (11c), and (12a)). The scattered *P*-polarized light field demonstrated a similar dependence on m_{0y}. On the contrary, the static magnetization component is included in the reflected *p*-polarized and scattered *S*-polarized field in the form of the first power, *i.e.* m_{0y} (Eqs. (11b), (11d), and (16)). The change of the intensity of the reflected *p*-polarized light with the magnetization reversal manifests itself in the so-called transverse MO Kerr effect [34]. It has been shown that the lateral shift of *p*-polarized light reflected from a YIG/GGG bilayer changes by less than 1% with the magnetization switching in the transverse MO configuration at the incidence angles around the reflectivity minimum [12]. At the reflection from the YIG/GGG interface around $\theta_{cr}^{(p)}$, the decrease of $\Delta x_p^{(\mathrm{ref})}$ is of the same order of magnitude. Similarly, upon $\mathbf{m}_0$ reversal, the scattered *S*-polarized field changes, and so does the GH shift. Indeed, upon the switch from $\mathbf{m}_0$ parallel to antiparallel to the *y*-axis, the maximum of $\Delta x_S^{(\mathrm{sc})}$ decreases by 2%.

Optical Materials EXPRESS

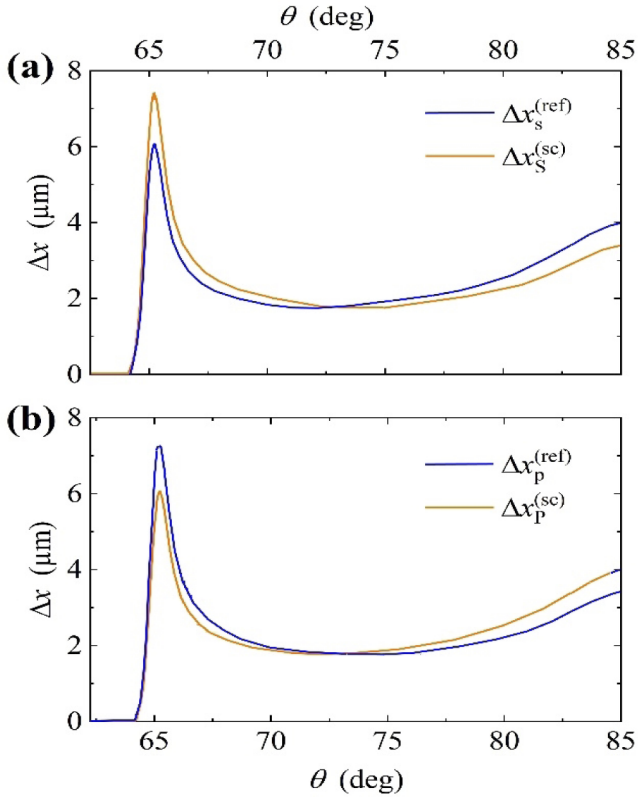

Fig. 3. The GH shift of *s*-polarized (a) and *p*-polarized (b) reflected light (blue lines) and scattered light (orange lines).

It should be noted that in the materials characterized by high values of gyromagnetic coefficients (such as, for instance, Bi-dopped YIG), the dependence of the tensor components of magnetic permeability on the magnetization cannot be neglected, which will lead to change of the *s*-polarized reflected light and *P*-polarized scattered light and the corresponding GH shifts with the magnetization reversal.

In addition to the magnetic field, the parameters of the spin wave also can be a controlling tool of the optical response of a magnetic system and thus can change the lateral shift of the scattered electromagnetic wave. The scattered field is proportional to the dynamical magnetization $\Delta\mathbf{m}$ (see Eqs. (14) and (16)), thus, the variation of the spin wave amplitude will only affect the amplitude of the scattered light and will not have an impact on the GH shift. On the contrary, the change of the frequency Ω of the spin wave will change both the amplitude and the shape of the scattered beam. Our calculations show that, for instance, at BLS by a spin wave of frequency $\Omega = 2\pi\cdot 40$ rad·GHz the GH shifts $\Delta x_S^{(sc)}$ and $\Delta x_P^{(sc)}$ increase by 1.4% and 0.8%, respectively, in comparison to the scattering by a spin wave of $\Omega = 2\pi\cdot 20$ rad·GHz discussed above. Such a different polarization-dependent tendency for the GH shift of the scattered light is related to the interplay between the linear and quadratic (by magnetization) elements of the MO tensors which affect the behavior of *s*- and *p*-polarized electromagnetic waves (see, for instance, Eq. (12)).

We can expect, that in multilayered systems, for instance, in photonic-magnonic crystals [15], the GH shift of the electromagnetic wave inelastically scattered by a spin wave can be increased up to several tens of the wavelength and can be efficiently controlled by the frequency of the spin wave.

Optical Materials EXPRESS

4. Conclusions

In conclusion, we have shown theoretically and numerically that at the Brillouin light scattering by a spin wave it is possible to observe the Goos-Hänchen effect — a spatial lateral shift of the reflected electromagnetic beam at the frequencies shifted by the frequency of the spin wave. We have shown that this effect is sensitive to the polarization state and the incidence angle of the light beam, namely, the Goos-Hänchen shift of the scattered light is larger for the *S*-polarization state than for the *P*-polarization state, and, similarly to the reflected light at the fundamental frequency, both these shifts reach maxima (about ten wavelengths) around the critical angles of incidence. Moreover, the Goos-Hänchen shift of the *S*-polarized scattered electromagnetic wave can be varied by the reversal of the static magnetization in the magnetic medium. Additionally, the change of the spin wave frequency leads to a small enhancement of the lateral shift, which can be increased in multilayered photonic systems. We hope that investigated phenomenon of lateral shift at the inelastic light scattering by magnons will be useful for the study of dynamical properties of magnetic materials and complex magnetic superstructures.

Funding. Collège de France, École Nationale d'Ingénieurs de Brest (Programme PAUSE); European Cooperation in Science and Technology (CA17123 "MAGNETOFON").

Disclosures. The authors declare that there are no conflicts of interest related to this article.

Data availability. Data underlying the results presented in this paper are not publicly available at this time but may be obtained from the authors upon reasonable request.

References

1. F. Goos and H. Hänchen, "Ein neuer und fundamentaler Versuch zur Totalreflexion," Ann. Phys. **436**(7-8), 333–346 (1947).
2. T. Tang, L. Luo, W. Liu, X. He, and Y. Zhang, "Goos–Hänchen effect in semiconductor metamaterial waveguide and its application as a biosensor," Appl. Phys. B **120**(3), 497–504 (2015).
3. Y. S. Dadoenkova, F. F. L. Bentivegna, V. V. Svetukhin, A. V. Zhukov, R. V. Petrov, and M. I. Bichurin, "Controlling optical beam shifts upon reflection from a magneto-electric liquid-crystal-based system for applications to chemical vapor sensing," Appl. Phys. B **123**(4), 107 (2017).
4. Y. S. Dadoenkova, F. F. L. Bentivegna, R. V. Petrov, and M. I. Bichurin, "Thermal dependence of the lateral shift of a light beam reflected from a liquid crystal cell deposited on a magnetic film," J. Appl. Phys. **123**(3), 033105 (2018).
5. A. Farmani, A. Mir, and Z. Sharifpour, "Broadly tunable and bidirectional terahertz graphene plasmonic switch based on enhanced Goos-Hänchen effect," Appl. Surf. Sci. **453**, 358–364 (2018).
6. H. Sattari, S. Ebadollahi-Bakhtevar, and M. Sahrai, "Proposal for a 1×3 Goos-Hänchen shift-assisted de/multiplexer based on a multilayer structure containing quantum dots," J. Appl. Phys. **120**(13), 133102 (2016).
7. A. Aiello, "Goos–Hänchen and Imbert–Fedorov shifts: a novel perspective," New J. Phys. **14**(1), 013058 (2012).
8. K. Y. Bliokh and A. Aiello, "Goos–Hänchen and Imbert–Fedorov beam shifts: an overview," J. Opt. **15**(1), 014001 (2013).
9. I. J. Singh and V. P. Nayyar, "Lateral displacement of a light beam at a ferrite interface," J. Appl. Phys. **69**(11), 7820–7824 (1991).
10. S. B. Borisov, N. N. Dadoenkova, I. L. Lyubchanskii, and M. I. Lyubchanskii, "Goos-Hänchen effect for the light reflected from the interface formed by bigyrotropic and nongyrotropic media," Opt. Spectrosc. **85**, 225–231 (1998).
11. T. Tang, J. Qin, J. Xie, L. Deng, and L. Bi, "Magneto-optical Goos-Hänchen effect in a prism-waveguide coupling structure," Opt. Express **22**(22), 27042–27055 (2014).
12. Y. S. Dadoenkova, F. F. L. Bentivegna, N. N. Dadoenkova, I. L. Lyubchanskii, and Y. P. Lee, "Influence of misfit strain on the Goos–Hänchen shift upon reflection from a magnetic film on a nonmagnetic substrate," J. Opt. Soc. Am. B **33**(3), 393 (2016).
13. Y. S. Dadoenkova, F. F. L. Bentivegna, N. N. Dadoenkova, R. V. Petrov, I. L. Lyubchanskii, and M. I. Bichurin, "Controlling the Goos-Hänchen shift with external electric and magnetic fields in an electro-optic/magneto-electric heterostructure," J. Appl. Phys. **119**(20), 203101 (2016).
14. Y. S. Dadoenkova, F. F. L. Bentivegna, N. N. Dadoenkova, R. V. Petrov, I. L. Lyubchanskii, and M. I. Bichurin, "Influence of the linear magneto-electric effect on the lateral shift of light reflected from a magneto-electric film," J. Phys.: Conf. Ser. **741**, 012201 (2016).
15. Y. S. Dadoenkova, N. N. Dadoenkova, J. W. Kłos, M. Krawczyk, and I. L. Lyubchanskii, "Goos-Hänchen effect in light transmission through biperiodic photonic-magnonic crystals," Phys. Rev. A **96**(4), 043804 (2017).
16. V. B. Silva and T. Dumelow, "Surface mode enhancement of the Goos-Hänchen shift in direct reflection off antiferromagnets," Phys. Rev. B **97**(23), 235158 (2018).

Optical Materials EXPRESS

17. B. Yu, T. Tang, R. Wang, S. Qiao, Y. Li, C. Li, J. Shen, X. Huang, and Y. Cao, "Magneto-optical and thermo-optical modulations of Goos-Hänchen effect in one-dimensional photonic crystal with graphene-VO_2," J. Magn. Magn. Mater. **530**, 167946 (2021).
18. T. Tang, J. Li, L. Luo, J. Shen, C. Li, J. Qin, L. Bi, and J. Hou, "Weak measurement of magneto-optical Goos-Hänchen effect," Opt. Express **27**(13), 17638–17646 (2019).
19. L. M. Brekhovskikh and O. A. Godin, *Acoustics of Layered Media II* 2nd ed. (Springer, 1999).
20. Y. S. Dadoenkova, N. N. Dadoenkova, I. L. Lyubchanskii, M. L. Sokolovskyy, J. W. Kłos, J. Romero-Vivas, and M. Krawczyk, "Huge Goos-Hänchen effect for spin waves: A promising tool for study magnetic properties at interfaces," Appl. Phys. Lett. **101**(4), 042404 (2012).
21. P. Gruszecki, J. Romero-Vivas, Yu. S. Dadoenkova, N. N. Dadoenkova, I. L. Lyubchanskii, and M. Krawczyk, "Goos-Hänchen effect and bending of spin wave beams in thin magnetic films," Appl. Phys. Lett. **105**(24), 242406 (2014).
22. X. Chen, X.-J. Lu, Y. Ban, and C.-F. Li, "Electronic analogy of the Goos–Hänchen effect: a review," J. Opt. **15**(3), 033001 (2013).
23. V. A. Bushuev and A. I. Frank, "Goos-Hänchen effect in neutron optics and the reflection time of neutron waves," Phys.-Usp. **61**(10), 952–964 (2018).
24. H. Shih and N. Blombergen, "Phase-matched critical total reflection and the Goos-Hänchen shift in second-harmonic generation," Phys. Rev. A **3**(1), 412–420 (1971).
25. V. J. Yallapragada, A. V. Gopal, and G. S. Agarwal, "Goos-Hänchen shifts in harmonic generation from metals," Opt. Express **21**(9), 10878–10885 (2013).
26. Y. S. Dadoenkova, N. N. Dadoenkova, M. Krawczyk, and I. L. Lyubchanskii, "Goos–Hänchen effect for Brillouin light scattering by acoustic phonons," Opt. Lett. **43**(16), 3965–3968 (2018).
27. M. G. Cottam and D. J. Lockwood, *Light Scattering in Magnetic Solids* (Wiley, 1986).
28. A. S. Borovik-Romanov and N. M. Kreines, "Brillouin-Mandelstam scattering from thermal and excited magnons," Phys. Rep. **81**(5), 351–408 (1982).
29. S. Demokritov and E. Tsymbal, "Light scattering from spin waves in thin films and layered systems," J. Phys.: Condens. Matter **6**(36), 7145–7188 (1994).
30. S. O. Demokritov, B. Hillebrands, and A. N. Slavin, "Brillouin light scattering studies of confined spin waves: linear and nonlinear confinement," Phys. Rep. **348**(6), 441–489 (2001).
31. S. A. Nikitov, D. V. Kalyabin, I. V. Lisenkov, A. N. Slavin, Yu. N. Barabanenkov, S. A. Osokin, A. V. Sadovnikov, E. N. Beginin, M. A. Morozova, Yu. P. Sharaevsky, Yu. A. Filimonov, Yu. V. Khivintsev, S. L. Vysotsky, V. K. Sakharov, and E. S. Pavlov, "Magnonics: a new research area in spintronics and spin wave electronics," Phys.-Usp. **58**(10), 1002–1028 (2015).
32. S. A. Nikitov, A. R. Safin, D. V. Kalyabin, A. V. Sadovnikov, E. N. Beginin, M. V. Logunov, M. A. Morozova, S. A. Odintsov, S. A. Osokin, A. Yu. Sharaevskaya, Yu Sharaevskaya, P. Sharaevsky, and A. I. Kirilyuk, "Dielectric magnonics: from gigahertz to terahertz," Phys.-Usp. **63**(10), 945–974 (2020).
33. F. Kargar and A. A. Balandin, "Advances in Brillouin–Mandelstam light-scattering spectroscopy," Nat. Photonics **15**(10), 720–731 (2021).
34. A. K. Zvezdin and V. A. Kotov, *Modern Magneto-Optics and Magneto-Optical Materials* (CRC Press, 1997).
35. R. W. Damon and J. R. Eshbach, "Magnetostatic modes of a ferromagnetic slab," J. Phys. Chem. Solids **19**(3-4), 308–320 (1961).
36. A. G. Gurevich and G. A. Melkov, *Magnetization Oscillations and Waves* (CRC Press, 1996).
37. D. D. Stancil and A. Prabahkar, *Spin Waves* (Springer, 2009).
38. Y. R. Shen, *The Principles of Nonlinear Optics* (Wiley, 1984).
39. K.-H. Landolt-Börnstein, A. M. Hellwege, and Hellwege, eds., *Group III, Condensed Matter, Vol. 12a, Magnetic and Other Properties of Oxides and Related Compounds - Part A: Garnets and Perovskites* (Springer-Verlag, 1978).

93.76.219.107 {ts '2022-01-26 18:27:26'}